



Dolomite utilization for removal of Zn²⁺ and Cu²⁺ ions from wastewater before determination by flame atomic absorption spectroscopy

Firas Fadhel Ali^a, Ahmed S. Al-Rawi^b, Abdulsalam M. Aljumaily^c, and Mohammed Oday Ezzat^{*a}

^a Department of Chemistry, Education College for Women, University of Anbar, Ramadi, Iraq

^b Department of Chemistry, College of Science, University of Anbar, Ramadi, Iraq

^c Department of Applied Chemistry, College of Applied Sciences, University of Fallujah, Fallujah, Iraq

ARTICLE INFO:

Received 12 Feb 2024

Revised form 16 Apr 2024

Accepted 15 May 2024

Available online 30 Jun 2024

Keywords:

Flame atomic absorption spectroscopy

Adsorption

Dolomite

Wastewater

Heavy metal ions

ABSTRACT

This study aims to use dolomite to remove Zn²⁺ and Cu²⁺ from wastewater. The adsorption process of the Zn²⁺ and Cu²⁺ was performed using the batch method at various factors (such as the amount of adsorbent, contact time, particle size, pH media, temperature, and initial concentration) to investigate the optimum removal conditions. The flame atomic absorption spectroscopy (F-AAS) was used to determine Zn²⁺ and Cu²⁺ after removal steps. The LOD of Zn²⁺ and Cu²⁺ were 0.05 mg L⁻¹ and 0.08 mg L⁻¹, respectively. Results showed that the adsorbent dolomite efficiently removed Zn²⁺ and Cu²⁺ with up to 98 % when 0.4 g of dolomite was used. The smaller dolomite particle size had higher removal efficiency for Zn²⁺ and Cu²⁺ ions. The results showed the removal of Zn²⁺ and Cu²⁺ was the maximum in the basic medium. Also, the removal of ions reached the maximum when dolomite had been in contact for 30 minutes with the wastewater. The experimental results of Langmuir and Freundlich adsorption isotherms show linearity where R² is more than (0.998 and 0.978) and (0.9915 and 0.9996) for Zn²⁺ and Cu²⁺, respectively. The maximum monolayer capacities (q_{max}) were obtained at 91.74 mg g⁻¹ for Cu²⁺ and 44.24 mg g⁻¹ for Zn²⁺.

1. Introduction

The decrease in the amount of rain around the world caused to decrease in the level of freshwater. On the other side, global freshwater demand is estimated to increase due to population growth and industrial development[1]. Therefore, it is very important to keep the water resources as clean as possible, whereby the contamination of resource water can lead to reducing accessible freshwater. The pollution of freshwater resources has become a serious problem that needs quick action before

it is too late to handle[2–5]. Developing current and new industries including but not limited to batteries, paper mills, board mills, fertilizers, petrochemicals, inorganic chemicals, basic steel works, basic non-ferrous metal works, motor vehicles, steam generation power plants, plating and painting has resulted in the release a significant amount of heavy metal ions such as lead, cadmium, chromium, copper and zinc that end up in the environment, especially in the water resource[6–8]. The increase in pollutants discharged into the water resource affects the amount of usable water and the ecosystem because of their high toxicity[9]. These pollutants must be removed from wastewater before they are released into the surface water.

*Corresponding Author: [Mohammed Oday Ezzat](mailto:mohammed.oday@uoanbar.edu.iq)

Email: edw.mohamed_oday@uoanbar.edu.iq

<https://doi.org/10.24200/amecj.v7.i02.311>

The researchers aim to find a way to reduce the release of pollutants into water resources [6,10]. Copper and zinc ions are considered toxic heavy metals. At the health-based guideline, copper and zinc concentrations in surface water that are below 2 mg L⁻¹ and 3 mg L⁻¹ respectively are deemed acceptable [9,11]. Thus, the concentration of heavy metals in wastewater should not exceed the maximum allowable concentration (MAC) before it is discharged to meet water quality guidelines. It is crucial to address the treatment of wastewater contaminated with heavy metals, which poses a significant challenge for industries [12]. Removal of heavy metal ions from wastewater can be accomplished by a variety of treatment methods including chemical methods such as precipitation, complexation, ion exchange, solvent extraction, and adsorption process by activated carbon and clay, and sieve process by membranes [1, 13, 14]. The use of an adsorption process to remove heavy metal ions from wastewater has recently achieved significant interest because it mainly depends on using environmentally friendly and economically effective materials as their adsorbents [3,15]. The heavy metal removal can be achieved by an adsorption process using minerals, which have essential properties that make them excellent adsorbents. The heightened capability to adsorb due to their high surface area, pores, and cavities are among these properties [16]. The minerals could also act as ion exchangers replacing the ions contained in their structure with the heavy metal ions in the wastewater [17,18]. These minerals can be easily collected as waste or side products from numerous industries at zero value, and they have to be an effective adsorbent. Minerals like dolomite powder, which is regarded as waste from the residual of the build processes. Furthermore, it can be a viable choice to be used as an adsorbent for the removal of heavy metals from wastewater [3,19]. This study aims to evaluate the potential ability of dolomite powder for removing of Zn²⁺ and Cu²⁺ from wastewater. Dolomite powder is naturally occurring rock produced in large amounts as a byproduct with low cost. So, the dolomite powder

is used as an adsorbent for removing Zn²⁺ and Cu²⁺ ions in water samples before being determined by F-AAS.

2. Materials and Methods

2.1. Materials

Both Zn²⁺ and Cu²⁺ stock solutions were prepared by dissolving 3.8019 g of Cu(NO₃)₂·3H₂O (CAS N.: 10031-43-3, Sigma, Germany) and 2.0849 g ZnCl₂ (CAS N.: 7646-85-7, Sigma, Germany) in 1 L of deionized water to get 1000 mg L⁻¹ as stock solutions. Hydrochloric acid (37%, CAS N.: 7647-01-0), Nitric acid (HNO₃, CAS N.: 7697-37-2), Ammonia-ammonium chloride buffer (CAS N.: 16052-06-5), sodium acetate-acetic acid buffer (pH 3.7-5.6, CAS N.: 126-96-5), Na₂HPO₄-NaH₂PO₄ buffer (pH 5.8-8.0, CAS N.: 7558-79-4) purchased from Sigma, Germany.

2.2. Preparation of adsorbent

The dolomite was obtained from the residual of the building processes. The dolomite was firstly dried overnight, milled, and sieved to unify particles size of three sizes of 150, 250, and 300 μm [19].

2.3. Apparatus

Field emission scanning electron emission with Energy dispersive spectroscopy (FE-SEM with EDX) was utilized for screening of the morphology of dolomite and component analysis using HITACHI S4500. The X-ray diffraction (XRD) was achieved on a Bruker D8 Advance (Cu Kα radiation, λ = 1.5406 nm) to study the structure of dolomite. Thermal gravimetric analysis (TGA) was achieved using a Rheometric Scientific STA 1500 instrument to measure water contents and thermal stability. Flame atomic absorption spectroscopy (FAAS) (Phoenix 986 AAS, USA) was used to determine the remaining concentration of Zn²⁺ and Cu²⁺ in the solution after the adsorption process was conducted.

2.4. Adsorption Procedure

The adsorption experiment was accomplished using the batch method. 0.4 g of dolomite was mixed with 50 mL of Zn²⁺ and Cu²⁺ solutions in a 100 mL polyethylene tube. The samples were shaken under

controlled conditions for a specific time between 15-120 min. The adsorption process was achieved at pH between 2 - 10, temperatures between 293 - 323°K, and initial concentrations between 50-100 mg L⁻¹[17, 19]. By separating, the dolomite was separated from the mixture via centrifugation. The last remaining concentration of Zn²⁺ and Cu²⁺ in the solution after the adsorption process was evaluated by flame atomic absorption spectroscopy (FAAS) by standard concentration between 0.1 and 1 mg L⁻¹ for both ions Zn²⁺ and Cu²⁺. The FAAS has a low detection limits (LOD) value, a limit of quantification (LOQ) value, and high selectivity, which make it the perfect apparatus for determining most heavy metal concentrations (Fig.1). The LOD of Zn²⁺ and Cu²⁺ were 0.05 mg L⁻¹ and 0.08 mg L⁻¹, respectively. The LOQ of Zn²⁺ and Cu²⁺ were evaluated at 0.18mg L⁻¹ and 0.25mg L⁻¹, respectively. The whole average relative standard deviation (RSD) was 3.6% and 5.6% for Zn²⁺ and Cu²⁺, respectively.

2.5. Adsorption Isotherms:

The relationship between the amount value of removed ions adsorbed and the amount value of dolomite at equilibrium conditions was

calculated using Equation 1 which was published by Vanderborght and Van Grieken[20]. The Hanes–Wolf as Equation 2 was applied to express the Langmuir isotherms at equilibrium conditions[2, 17, 18]. The Freundlich adsorption model was used as another absorption model (Eq. 3). This model is useful to indicate that the adsorption energy value on a homogeneous surface is independent of surface coverage, according to the Equation 3[17]. The Temkin model has been shown by the Equations 4 and 5 [21].

$$q_e = (C_o - C_e) * V/m$$

(Eq.1)

Where q_e =Quantity (mg g⁻¹) of ion adsorbed on the dolomite at equilibrium conditions, C_o =Initial concentration (mg L⁻¹) of the ion, C_e =Concentration (mg L⁻¹) at equilibrium conditions, m = Mass (g) of adsorbent and V =Volume of the solution

$$C_e/q_e = 1/(K_L * q_m) + (1/q_m) * C_e$$

(Eq.2)

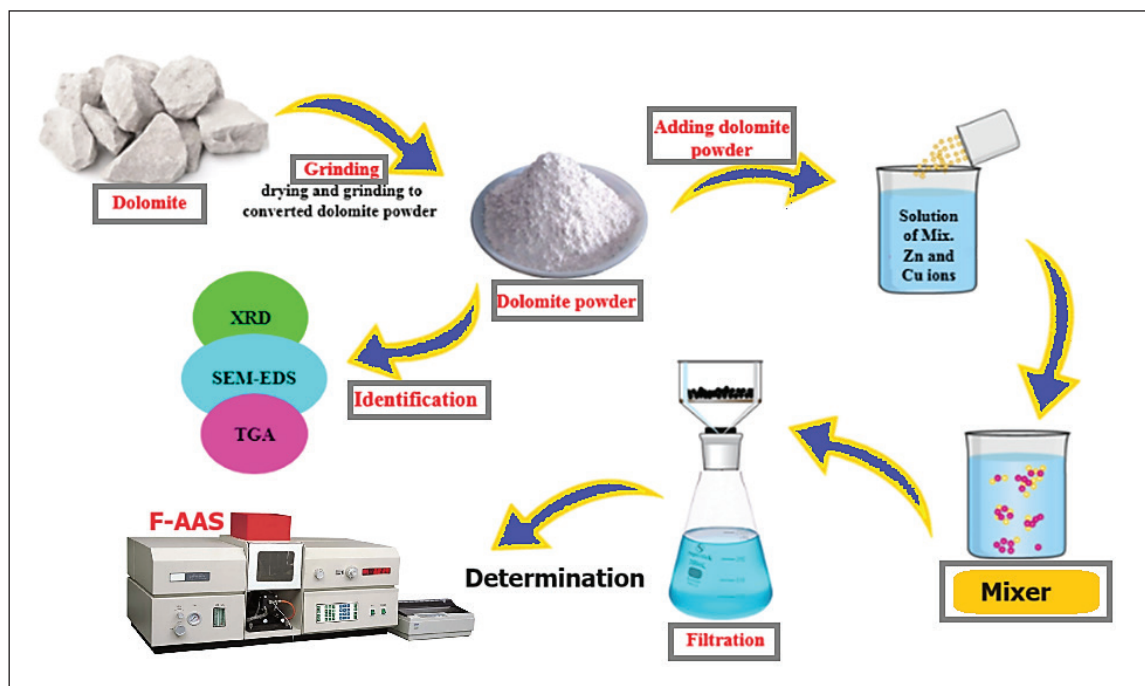


Fig. 1. The Zn²⁺ and Cu²⁺ removal/adsorption based on dolomite before determined by F-AAS

where q_{\max} (mg g⁻¹) = The maximum amount value of ions adsorbed on the dolomite surface, leading to creating a monolayer of ions on the surface of dolomite, and K_L = The Langmuir constant corresponding to the adsorption energy value. The value of q_{\max} was calculated from the slope and K_L was calculated from the crossing intercept of the plot of C_e/q_e against C_e .

$$q_e = K_f C_e^{1/n} \quad (\text{Eq. 3})$$

where K_f = Freundlich model constant (mg g⁻¹), n = Adsorption intensity, C_e = The remaining concentration (mg L⁻¹) at equilibrium, q_e = The quantity (mg g⁻¹) of ion adsorbed onto dolomite at equilibrium [17,18].

$$q_e = B \ln A_T + B \ln C_e \quad (\text{Eq. 4})$$

$$b_T = RT/b \quad (\text{Eq. 5})$$

where B = Constant related to heat of sorption (Jmol⁻¹), b_T = Temkin model constant, A_T = Temkin

model equilibrium binding constant (L g⁻¹), q_e = the quantity (mg g⁻¹) of ion adsorbed onto dolomite at equilibrium, R = Universal gas constant (8.314 Jmol⁻¹K⁻¹) and T = Temperature at 298°K.

3. Results and Discussion

3.1. Characterization of the synthesized materials

Scanning electron microscopy (SEM) was used to image the morphology of the dolomite. From the SEM images of dolomite shown in Figure 2, it was observed that the morphology of dolomite consists of irregularly shaped particles with rough surfaces[22]. The XRD patterns of dolomite powder are shown in Figure 3. The results indicate that dolomite powder mainly consists of dolomite[23]. These results are consistent with the EDX spectrum shown in Table 1. EDX spectrum was used to study the components of dolomite. The results illustrated in Table 1 show that the dolomite is dominated by oxygen at ~ 41%, calcium at ~ 36%, and carbon at 22%[22].

The TGA (Fig. 4) shows weight loss at ~ 600°C suggesting the release of CO₂ from the decomposition of dolomite (CaCO₃)[23]. The reaction can be described by Equation 6.

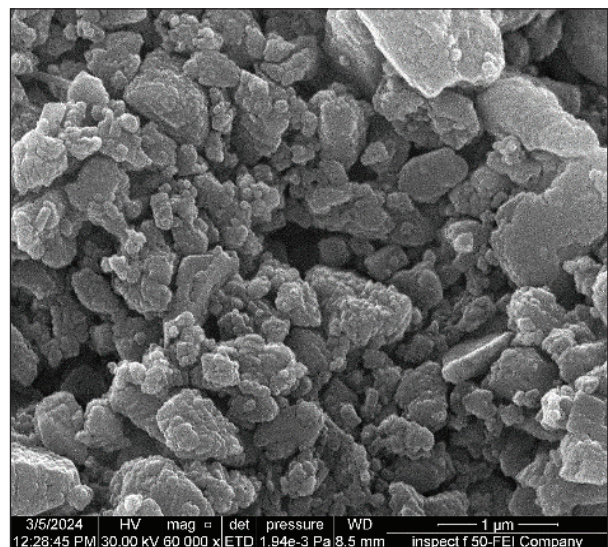
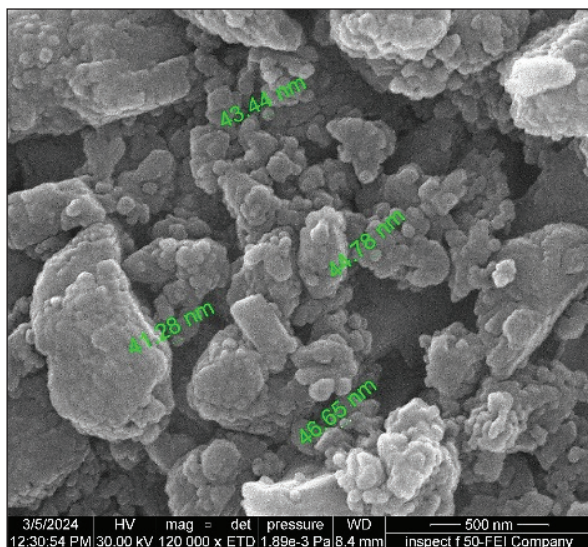
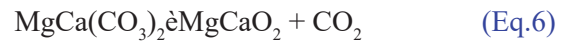


Fig. 2. SEM images of dolomite

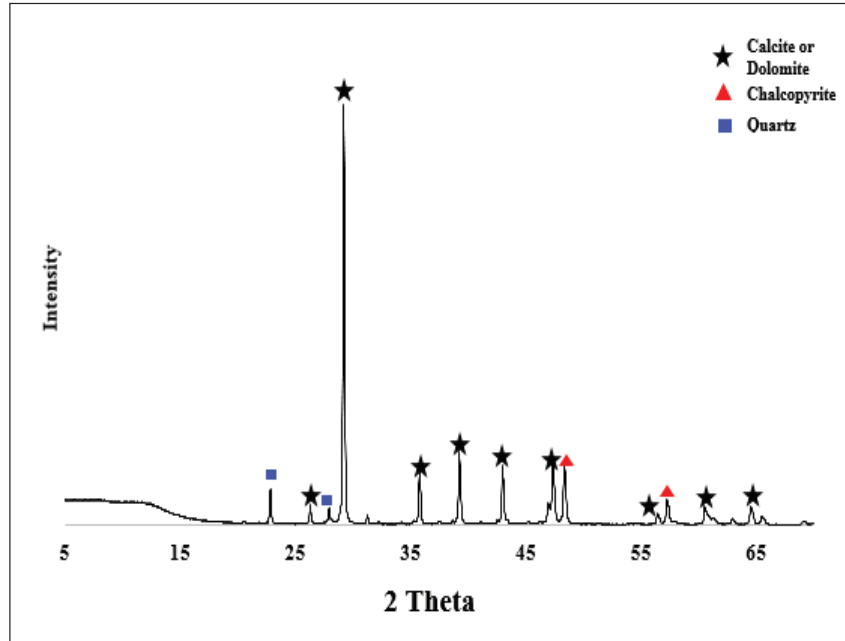


Fig.3.XRD of the dolomite

Table 1. The elemental analysis of dolomite

Element	Weight %
C	14.4
O	47.37
Mg	0.51
Al	0.25
Si	0.55
Ca	36.93
Total	100.00

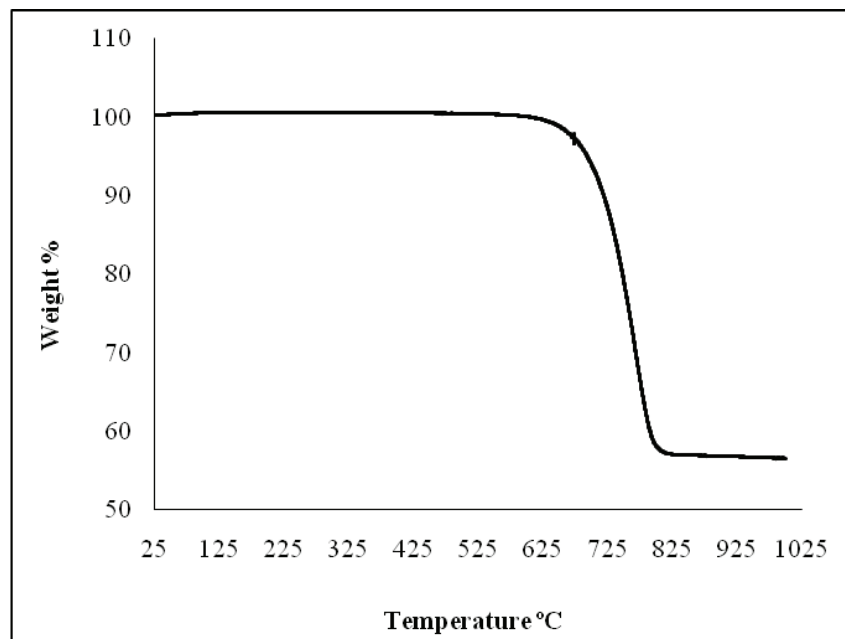


Fig.4.TGA of the dolomite

3.2. Adsorption study

3.2.1. Effect of dolomite amounts

A variety of dolomite amounts at 0.2, 0.4, 0.6, 0.8, and 1 g were used to remove of Zn²⁺ and Cu²⁺ as shown in Figure 5. The dolomite adsorption capacity for the removal of Zn²⁺ was around 82% when an amount of 0.2 g of dolomite was used. The adsorption capacity sharply increases up to 98% when the dolomite amount is increased to 0.4 g. On the other side, the adsorption capacity for the removal of Cu²⁺ was around 86% when 0.2 g of the dolomite was used. This adsorption capacity for the removal of Cu²⁺ was increased to 98% when the dolomite amount was increased to 0.4 g. The adsorption capacity for the removal of Zn²⁺ and Cu²⁺ showed no noticeable increase when the dolomite amount increased up to 1.0 g. According to these results, the 0.4 g of dolomite amount would be used to investigate other adsorption factors [24].

3.2.2. Contact time effect

The adsorption capacity for Zn²⁺ and Cu²⁺ was measured as an indicator for determining the optimum contact time for the removal of Zn²⁺ and Cu²⁺ by dolomite. The adsorption results obtained at

25°C for Zn²⁺ and Cu²⁺ have the same trend as shown in Figure 6. The results implicate that the adsorption on the dolomite increased rapidly when the time was increased from 15 min to 30 min after the adsorption became almost constant. The maximum removal of Zn²⁺ and Cu²⁺, around 98.5%, was achieved after 30 min, and so, equilibrium was reached, where no noticeable change in the adsorption was observed. The contact time was kept to 120 min [24, 25].

3.2.3. Effect of pH

The pH of solution at which the adsorption process would take place is an important factor that affects the efficiency of adsorption. The pH can influence the solubility of the ions to be removed. It can also affect the charge of function group onto the surface of the adsorbent. This study investigated the adsorption at a range of pH between 2 and 10, time of 30 min, weight of adsorbent of 0.4 g, and size of particles of 150 µm. The removal percentage of Zn²⁺ and Cu²⁺ at the chosen range of pH is illustrated in Figure 7. At a lower pH of 2, the removal percentage of the Zn²⁺ was 80% because metal ions were hindered by hydrogen ions that occupied active sites available on the adsorbent surface and competed with the metal ions.

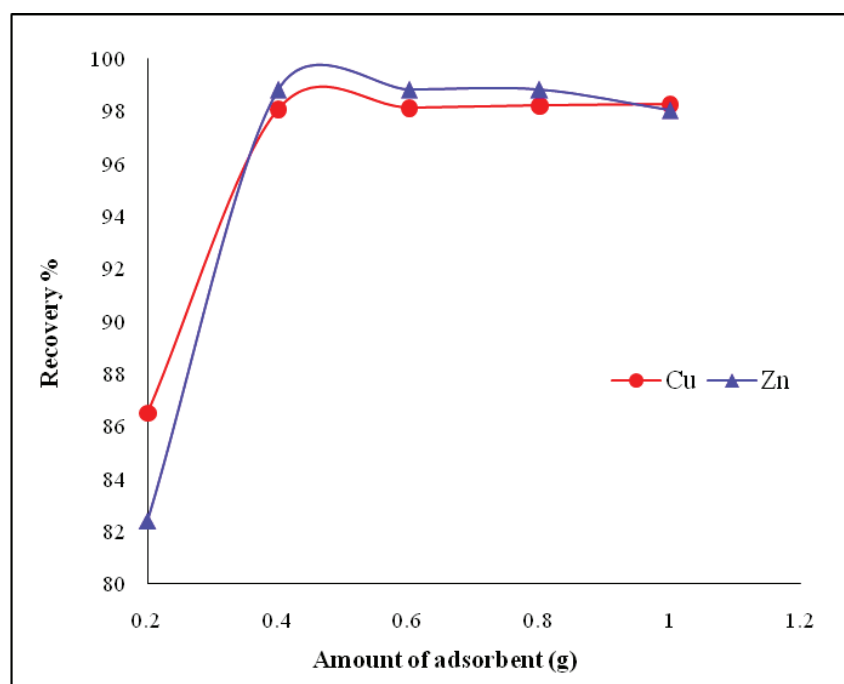


Fig. 5. The effect of dolomite amounts on Zn²⁺ and Cu²⁺ removal

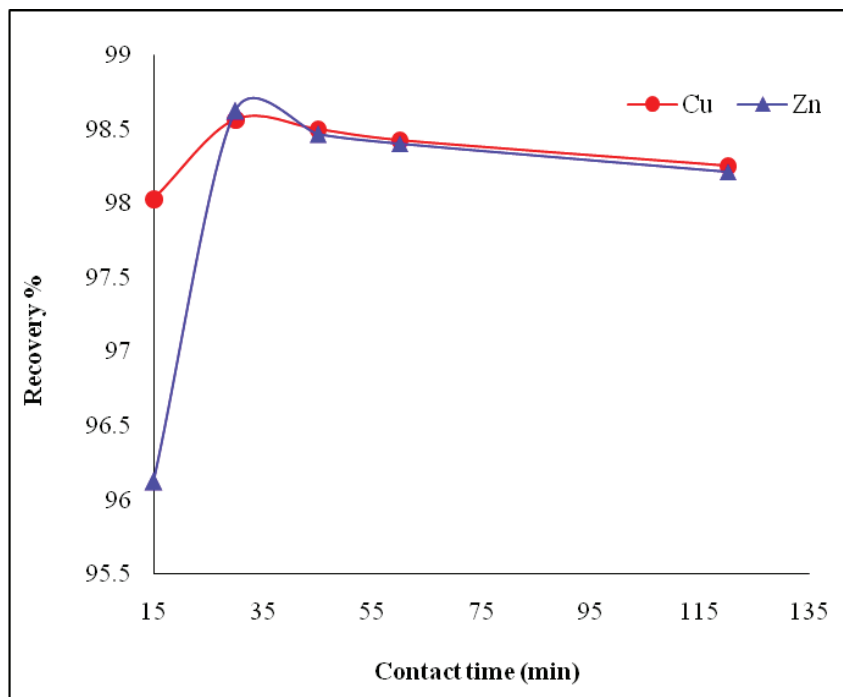


Fig. 6. The effect of time on the removal of Zn²⁺ and Cu²⁺ at 293K using dolomite as adsorbent

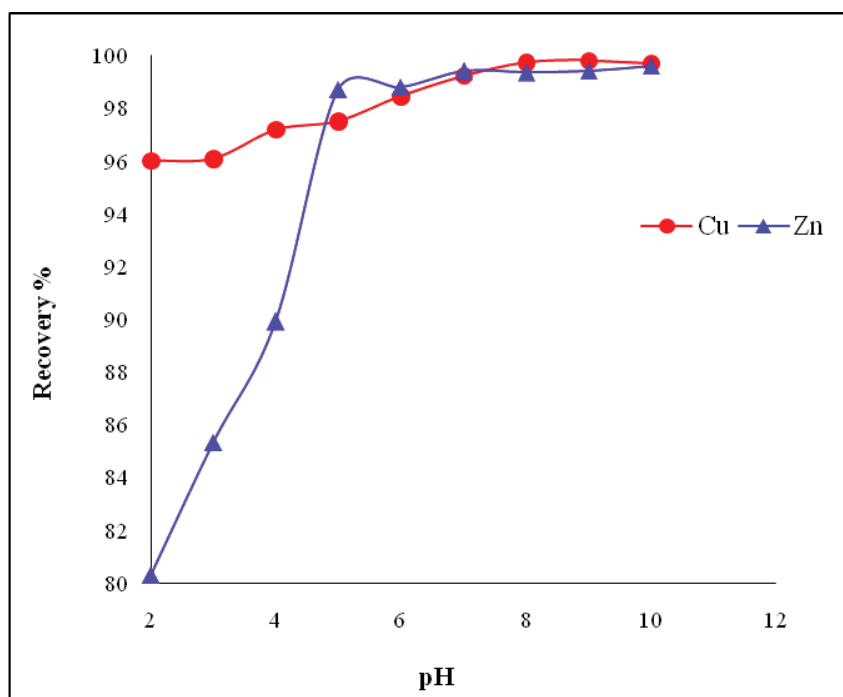


Fig. 7. The effect of pH on the removal of Zn²⁺ and Cu²⁺ using dolomite as adsorbent

As the pH increased, the removal percentage of the Zn²⁺ increased due to reducing the concentration of hydrogen ions in the solution and setting free the active site onto the adsorbent surface. The removal percentage reached 98.7% at a pH of 5, and no

significant increase in the removal was observed at higher pH. The change of pH showed a slight effect on the removal of Cu²⁺ whereby the removal percentage also increased as the pH increased from 96% at a pH of 2 to 99.3% at a pH of 8 [10, 24, 26].

3.2.4. Effect of dolomite particle size

The effect of dolomite particles size was studied, and thus three sizes of the dolomite were investigated 150, 250 and 300 μm ., and the results are illustrated in Figure 8. It can be noticed that the adsorption capacity of Zn²⁺ and Cu²⁺ did not change when the particle size increased from 150 to 250 μm for both ions (Zn²⁺ and Cu²⁺). On the other side, using dolomite at 300 μm showed a slight decrease in the adsorption capacity for Cu²⁺ owing to the reduction of the surface area of the dolomite. This result confirmed that decreasing the particle size leads to an increase in the surface area of the dolomite powder and simultaneously increases the removal capability of ions [10, 27].

3.2.5. Effect of adsorption temperature

The effect of solution temperature (293, 303, 313, and 323°K) on the adsorption process was studied and shown in Figure 9. Temperature was shown to have a noticeable effect on the adsorption capacity of the Zn²⁺ and Cu²⁺. The adsorption capacity of dolomite for Zn²⁺ showed a slight decrease from 98.6% to 98.3% as the temperature increased from 293 to 323°K. On the other hand, the dolomite adsorption capacity for Cu²⁺ decreased from 98.4% to 97.3% when

the temperature increased from 293 to 323°K. These results confirmed that the adsorption is an exothermic process [28, 29].

3.2.6. Effect of initial concentration

The adsorption capacities of Zn²⁺ and Cu²⁺ onto the dolomite at various initial concentrations of the ions between 50–100 mg L⁻¹ are shown in Figure 10. It can be noticed that the adsorption capacity of Zn²⁺ and Cu²⁺ did not change and the adsorption capacity was almost the same for both ions. During the adsorption process, the initial concentration of targeted ions in the solution played a key role that limited the capacity of the adsorbent [30, 31]. Using the dolomite as an adsorbent for the removal of Zn²⁺ and Cu²⁺ showed that the adsorption capacity was kept constant as high as 98.6% for Zn²⁺ and Cu²⁺ with a very slight decrease for the adsorption capacity of Zn²⁺ to 97.8% when the initial concentration increased from 50 to 100 mg L⁻¹. Increasing the initial concentration from 50 to 100 mg L⁻¹ while the adsorption capacity was maintained as high as 98.8% confirms that the adsorbent did not reach the saturation point, and the initial concentration can be increased, where the adsorption capacity of Cu²⁺ was retained at 98.6% even though the concentration raised to 100 mg L⁻¹ [30, 31].

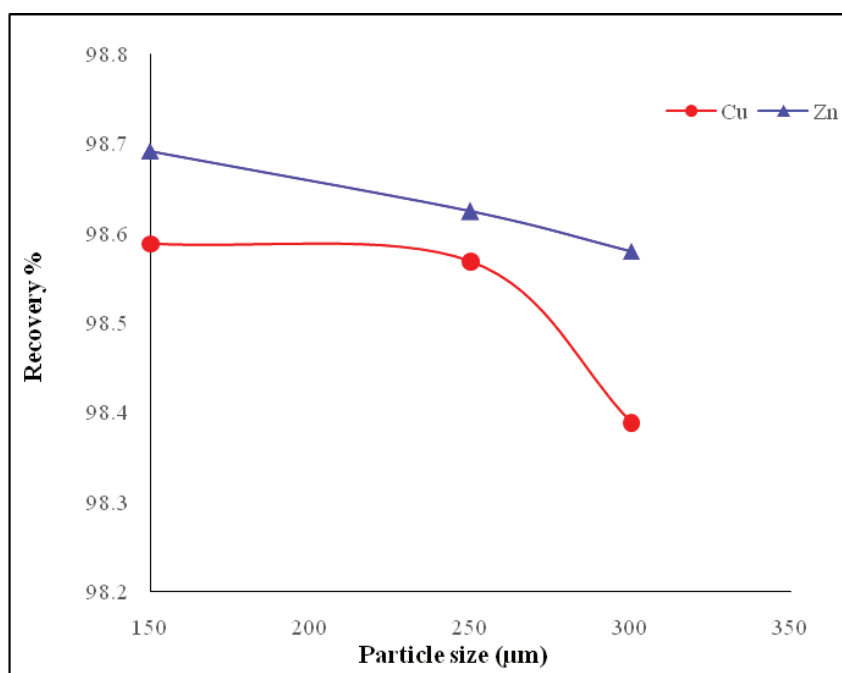


Fig. 8. The effect of dolomite particle size on the removal of Zn²⁺ and Cu²⁺

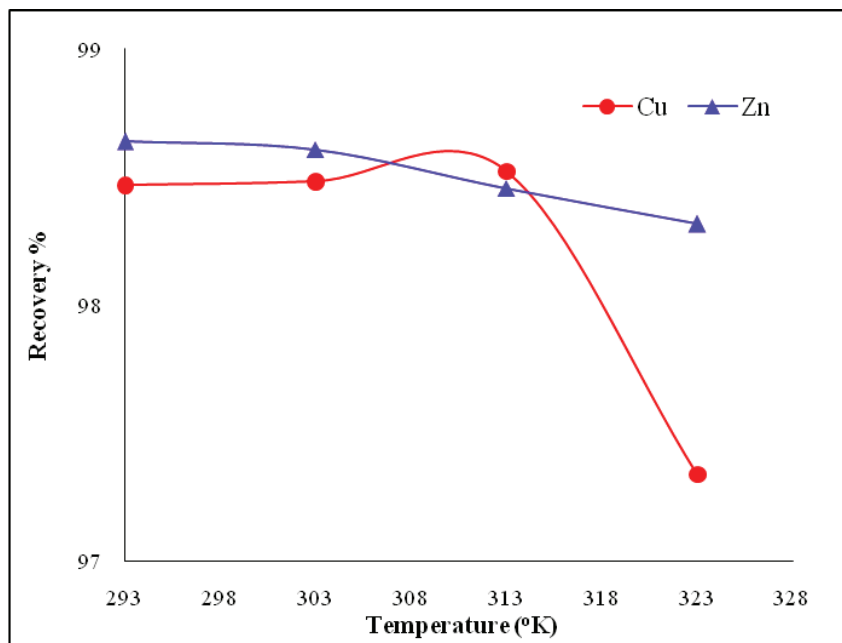


Fig. 9. The effect of temperature on the removal of Zn²⁺ and Cu²⁺

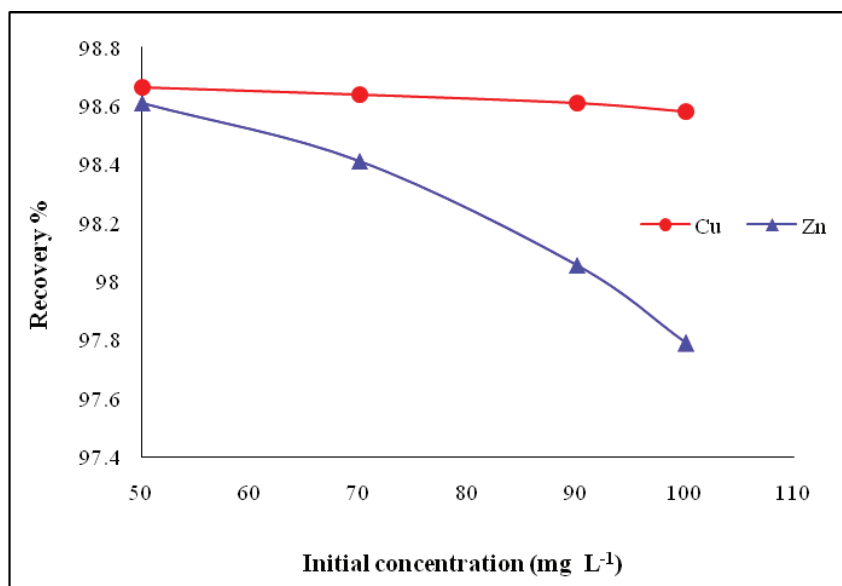


Fig. 10. The effect of initial concentration on the removal of Zn²⁺ and Cu²⁺

3.2.7. Isotherm model

The adsorption experiments were conducted to determine the extent of corresponding with Langmuir, Freundlich, and Timken models at optimum conditions of (dolomite amount 0.4 g, time 30 min, initial Zn²⁺ and Cu²⁺ concentration 50, 70, 90, and 100 mg L⁻¹ and pH 8). The association between the amounts of ions removed by the dolomite at equilibrium conditions was determined using the

procedure illustrated in the experiment and materials section [17], [32–35]. According to the Langmuir isotherm models; the Hanes–Woolf equation has been used and the results are shown in Figure 11. The correlation coefficient value summarized in Table 2 and obtained via this equation was up to 0.998 and 0.978 for Zn²⁺ and Cu²⁺ respectively. This suggests that the adsorption process is conformable with the Langmuir model and the Zn²⁺ and Cu²⁺ adsorbed onto

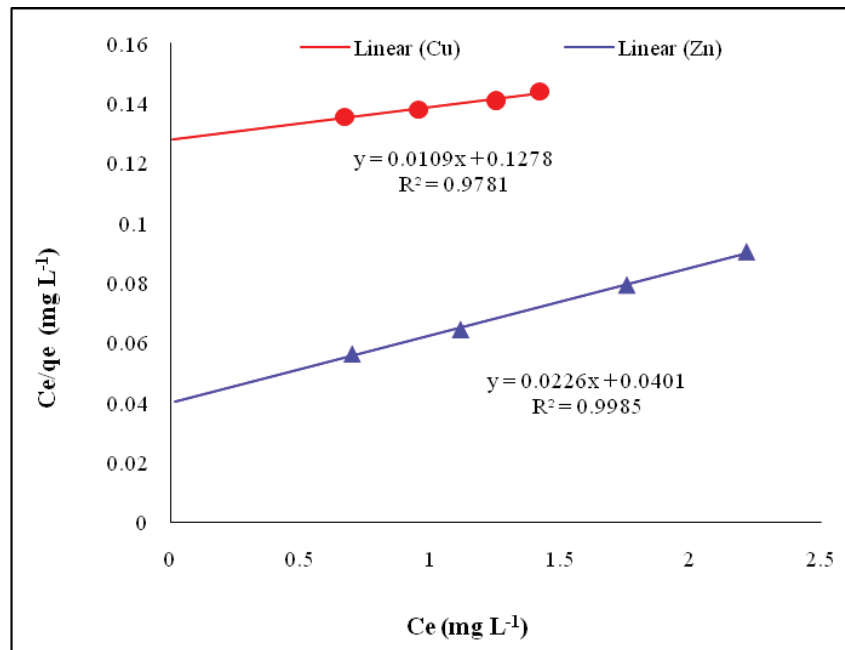


Fig. 11. Langmuir model at 293°K

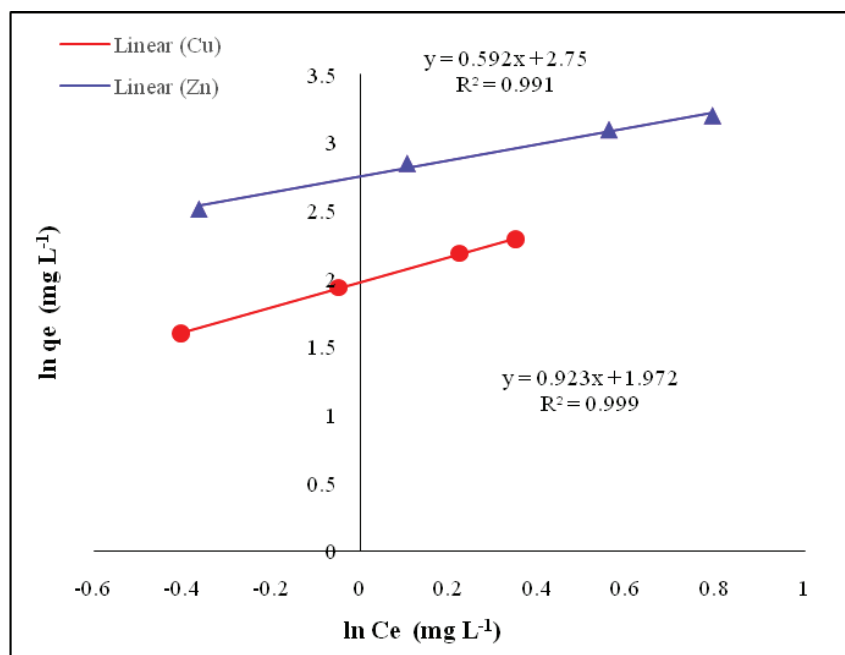


Fig. 12. Freundlich model at 293°K

the dolomite surface initially formed a monolayer [32], [35]. The maximum monolayer capacities of Zn²⁺ and Cu²⁺ adsorbed onto the dolomite obtained by the Langmuir model are 44.24 and 91.74 (mg g⁻¹), respectively, as summarized in Table 2.

The Freundlich isotherm model obtained using equation 3 is shown in Figure 12. The Freundlich isotherm showed good linearity where the

correlation coefficient (R^2) was 0.9915 and 0.9996 for Zn²⁺ and Cu²⁺, respectively, as summarized in Table 2. This confirms the multilayer adsorption of removed ions onto the dolomite surface and the obtained adsorption results agree with the Freundlich adsorption isotherm model [21, 36–38]. The K_f is an estimated indicator for the adsorption capacity, while $1/n$ refers to the adsorption strength.

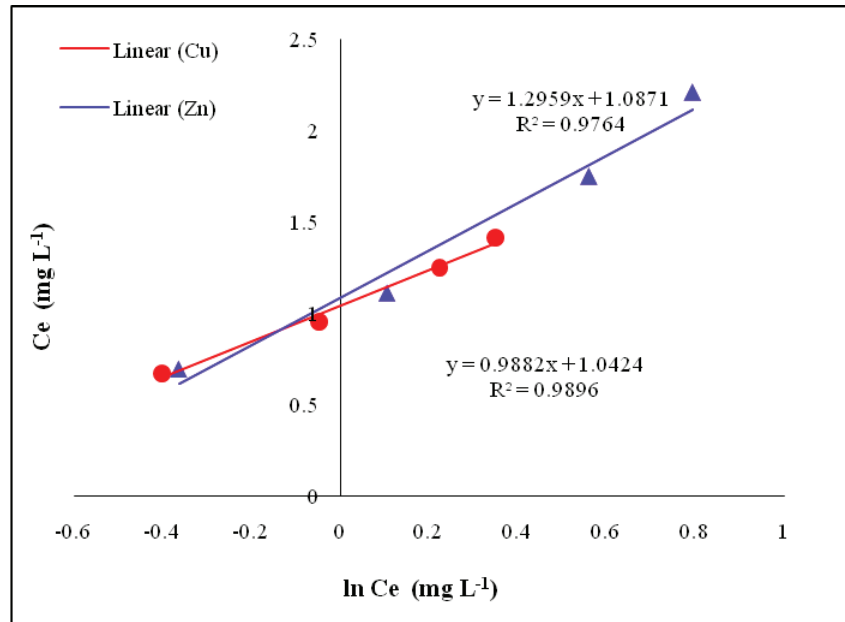


Fig. 13. Timken model at 293 K

Table 2. Adsorption models of Zn²⁺ and Cu²⁺ onto the dolomite

Ion	Model	Equation	Constant	Value
Cu	Langmuir	$C_e/q_e = 1/(K_L q_{max}) + (1/q_m) C_e$	R ²	0.997
			q _{max} (mg g ⁻¹)	91.743
			K _L (L mg ⁻¹)	0.085
	Freundlich	$q_e = K_f C_e^{1/n}$	R ²	0.999
			n	1.082
			1/n	0.923
			K _f (mg g ⁻¹)	-0.679
	Timken	$q_e = B \ln A_T + B \ln C_e$ $b_T = RT/B$	R ²	0.989
			B J mol ⁻¹	0.988
			A _T (L g ⁻¹)	2.871
Zn	Langmuir	$C_e/q_e = 1/(K_L q_{max}) + (1/q_m) C_e$	R ²	0.999
			q _{max} (mg g ⁻¹)	44.247
			K _L (L mg ⁻¹)	0.563
	Freundlich	$q_e = K_f C_e^{1/n}$	R ²	0.991
			n	1.687
			1/n	0.592
			K _f (mg g ⁻¹)	-1.011
	Timken	$q_e = B \ln A_T + B \ln C_e$ $b_T = RT/B$	R ²	0.976
			B J mol ⁻¹	1.295
			A _T (L g ⁻¹)	2.313
			b _T	1911.85

When $1/n$ is equal to 1, the separation between the two phases is independent of the concentration. If the value of $1/n$ is higher than 1, this indicates normal adsorption. When $1/n$ is lower than 1, this implies cooperative adsorption. According to the adsorption results summarized in Table 2, the value of $1/n$ of Zn²⁺ and Cu²⁺ = 0.592 and 0.923 while $n = 1.687$ and 1.082 respectively, indicating that the sorption of Zn²⁺ and Cu²⁺ onto dolomite is favorable [21, 36–38].

The R² values summarized in Table 2 were 0.976 and 0.989 for Zn²⁺ and Cu²⁺, respectively. They were obtained by fitting the adsorption experimental results to the Temkin model. Figure 13 shows that not all the plotted points of both ions were linear together. These findings suggest that the Langmuir and Freundlich models are highly convenient for predicting Zn²⁺ and Cu²⁺ adsorption onto the dolomite surface in comparison with the Temkin model. From the Temkin plot, the following values were estimated for Zn²⁺ and Cu²⁺: $A_T = 2.313 \text{ Lg}^{-1}$, $B = 1.295 \text{ Jmol}^{-1}$, and $A_T = 2.871 \text{ Lg}^{-1}$, $B = 0.988 \text{ Jmol}^{-1}$ respectively which represents the heat of adsorption suggesting a physisorption process [33, 35, 39, 40].

4. Conclusion

In this paper, an investigation of the removal of Zn²⁺ and Cu²⁺ was carried out using dolomite as an adsorbent. This adsorption capacity was up to 98% when the amount of dolomite was 0.4 g. The amount of adsorption onto dolomite powder was slightly higher for Cu²⁺ compared to Zn²⁺ from wastewater, where the maximum monolayer capacities (q_{max}) was 91.74 mg g⁻¹ for Cu²⁺ ion and 44.24 mg g⁻¹ for Zn²⁺. The value of $1/n$ and n for zinc and copper was obtained (0.592, 0.923) and (1.687, 1.082), respectively, indicating that the adsorption of zinc and copper onto dolomite is favorable. The experimental results agreed with the Langmuir, Freundlich, and Temkin model. The comparison between the three models shows that the Langmuir and Freundlich models have the highest correlation coefficient value of 0.998 compared with the Temkin model. It could be concluded that dolomite is an active adsorbent for the removal of Zn²⁺ and

Cu²⁺ from wastewater.

5. Acknowledgment

The authors appreciate the support of the University of Anbar/College of Science and College of Education for Women and the University of Fallujah/ College of Applied Sciences. The authors wish to thank the service research lab in the Chemistry Department, College of Science.

6. References

- [1] N. Abdullah, N. Yusof, W. J. Lau, J. Jaafar, A. F. Ismail, Recent trends of heavy metal removal from water/wastewater by membrane technologies, *J. Ind. Eng. Chem.*, 76 (2019) 17–38. <https://doi.org/10.1016/j.jiec.2019.03.029>
- [2] S. Ahmadi, C. A. Igwegbe, Adsorptive removal of phenol and aniline by modified bentonite: adsorption isotherm and kinetics study, *Appl. Water Sci.*, 8 (2018) 170. <https://doi.org/10.1007/s13201-018-0826-3>
- [3] F. F. Ali, A. S. Al-Rawi, A. M. Aljumaily, Limestone residues of sculpting factories utilization as sorbent for removing Pb (II) ion from aqueous solution, *Results Chem.*, 4 (2022) 100621. <https://doi.org/10.1016/j.rechem.2022.100621>
- [4] M. Karnib, A. Kabbani, H. Holail, Z. Olama, Heavy metals removal using activated carbon, silica and silica activated carbon composite, *Energy Procedia*, 50(2014) 113–120. <https://doi.org/10.1016/j.egypro.2014.06.014>
- [5] K. Atkovska, K. Lisichkov, G. Ruseska, A. T. Dimitrov, A. Grozdanov, Removal of heavy metal ions from wastewater using conventional and nanosorbents: a review, *J. Chem. Technol. Metall.*, 53 (2018) 202–219. https://journal.uctm.edu/node/j2018-2/7_17-59_A_Grozdanov_p_202_217.pdf
- [6] M. Yari, Removal of Pb (II) ion from aqueous solution by graphene oxide and functionalized graphene oxide-thiol: effect of cysteamine concentration on the bonding constant, *Desalin. Water Treat.*, 57 (2016) 11195–11210. <https://doi.org/10.1080/19443>

- 994.2015.1043953
- [7] O. Moradi, M. Aghaie, K. Zare, M. Monajjemi, H. Aghaie, The study of adsorption characteristics Cu²⁺ and Pb²⁺ ions onto PHEMA and P (MMA-HEMA) surfaces from aqueous single solution, *J. Hazard. Mater.*, 170 (2009) 673–679. <https://doi.org/10.1016/j.jhazmat.2009.05.012>
- [8] A. S. Al-Rawi, A. M. Aljumaily, W. M. Saod, E. A. Al-Heety, Pollution Level and Sources of Heavy Metals in Indoor Dust from College of Science, University of Anbar Campus, Iraq, in *IOP Conference Series: Earth Environ. Sci.*, IOP Publishing, 1300 (2024) 012019. <https://doi.org/10.1088/1755-1315/1300/1/012019>
- [9] WHO, Guidelines for drinking-water quality, World Health Organization, 2022. <https://www.who.int/publications/item/9789240045064>
- [10] H. Çelebi, G. Gök, O. Gök, Adsorption capability of brewed tea waste in waters containing toxic lead (II), cadmium (II), nickel (II), and zinc (II) heavy metal ions, *Sci. Reports*, 10 (2020) 17570. <https://doi.org/10.1038/s41598-020-74553-4>
- [11] F. Edition, Guidelines for drinking-water quality, 4th ed, World Health Organization, 38 (2011) 104–108. <https://www.scirp.org/reference/referencespapers?referenceid=3088676>
- [12] T. Zhang, Removal of heavy metals and dyes by clay-based adsorbents: From natural clays to 1D and 2D nano-composites, *Chem. Eng. J.*, 420 (2021) 127574. <https://doi.org/10.1016/j.cej.2020.127574>
- [13] A. Khaligh, F. Golbabaie, A. Vahid, On-line micro column preconcentration system based on amino bimodal mesoporous silica nanoparticles as a novel adsorbent for removal and speciation of chromium (III, VI) in environmental samples, *J. Environ. Health Sci. Eng.*, 13 (2015) 47. <https://doi.org/10.1186/s40201-015-0205-z>
- [14] A.A.M. Beigi, MM Eskandari, B Kalantari, Dispersive liquid-liquid microextraction based on task-specific ionic liquids for determination and speciation of chromium in human blood, *J. Anal. Chem.*, 70 (2015) 1448-1455. <https://doi.org/10.1134/S1061934815120072>
- [15] M.K. Abbasabadi, F Hosseini, Nanographene oxide modified phenyl methanethiol nanomagnetic composite for rapid separation of aluminum in wastewaters, foods, and vegetable samples by microwave dispersive magnetic micro solid-phase extraction, *Food Chem.*, 347(2021)129042. <https://doi.org/10.1016/j.foodchem.2021.129042>
- [16] MM Eskandari, Cloud point assisted dispersive ionic liquid-liquid microextraction for chromium speciation in human blood samples based on isopropyl 2-[(isopropoxycarbothioly) disulfanyl] ethane thioate, *Anal. Chem. Res.*, 10 (2016) 18-27. <https://doi.org/10.1016/j.ancr.2016.10.002>
- [17] S. Sen Gupta, K. G. Bhattacharyya, Interaction of metal ions with clays: I. A case study with Pb (II), *Appl. Clay Sci.*, 30 (2005) 199–208. <https://doi.org/10.1016/j.clay.2005.03.008>
- [18] A. A. El-Bayaa, N. A. Badawy, E. Abd AlKhalik, (2009) Effect of ionic strength on the adsorption of copper and chromium ions by vermiculite pure clay mineral, *J. Hazard. Mater.*, 170 (2009) 1204–1209. <https://doi.org/10.1016/j.jhazmat.2009.05.100>
- [19] A. S. Yahya, Study affecting factors on the recovery of some heavy metal ions from aqueous solutions using natural clay, *J. Univ. Anbar Pure Sci.*, 10 (2016) 76-82. <https://doi.org/10.37652/JUAPS.2016.135145>
- [20] B. M. Vanderborght, R. E. Van Grieken, Enrichment of trace metals in water by adsorption on activated carbon, *Anal. Chem.*, 49 (1977) 311–316. <https://doi.org/10.1021/ac50010a032>
- [21] B. Abbou, Kinetic and thermodynamic study on adsorption of cadmium from aqueous solutions using natural clay, *J. Turk. Chem.*

- Soc. Section A: Chem., 8 (2021) 677–692. <https://doi.org/10.18596/jotcsa.882016>
- [22] H. Yang, Calcined dolomite: an efficient and recyclable catalyst for synthesis of α , β -unsaturated carbonyl compounds, *Catal. Lett.*, 149 (2019) 778–787. <https://doi.org/10.1007/s10562-018-2632-9>
- [23] S. Medina-Carrasco, J. M. Valverde, In situ XRD analysis of dolomite calcination under CO₂ in a humid environment, *Cryst. Eng. Comm.*, 22 (2020) 6502–6516. <https://doi.org/10.1039/D0CE00974A>
- [24] H. Gebretsadik, A. Gebrekidan, L. Demlie, Removal of heavy metals from aqueous solutions using *Eucalyptus Camaldulensis*: An alternate low cost adsorbent, *Cogent Chem.*, 6 (2022) 1720892. <https://doi.org/10.1080/23312009.2020.1720892>
- [25] H. Hernández-Cocoletzi, Natural hydroxyapatite from fishbone waste for the rapid adsorption of heavy metals of aqueous effluent, *Environ. Technol. Inno.*, 20 (2020) 101109. <https://doi.org/10.1016/j.eti.2020.101109>
- [26] Z. Deng, Modification of coconut shell-based activated carbon and purification of wastewater, *Adv. Compos. Hybrid Mater.*, 4 (2021) 65–73. <https://doi.org/10.1007/s42114-021-00205-4>
- [27] B. Yu, Y. Zhang, A. Shukla, S. S. Shukla, K. L. Dorris, The removal of heavy metal from aqueous solutions by sawdust adsorption—removal of copper, *J. Hazard. Mater.*, 80 (2000) 33–42. [https://doi.org/10.1016/S0304-3894\(00\)00278-8](https://doi.org/10.1016/S0304-3894(00)00278-8)
- [28] S. Wadhawan, A. Jain, J. Nayyar, S. K. Mehta, Role of nanomaterials as adsorbents in heavy metal ion removal from waste water: A review, *J. Water Process Eng.*, 33 (2020) 101038. <https://doi.org/10.1016/j.jwpe.2019.101038>
- [29] G. Sarojini, S. Venkateshbabu, M. Rajasimman, Facile synthesis and characterization of polypyrrole-iron oxide–seaweed (PPy-Fe₃O₄-SW) nanocomposite and its exploration for adsorptive removal of Pb (II) from heavy metal bearing water, *Chemosphere*, 278 (2021) 130400. <https://doi.org/10.1016/j.chemosphere.2021.130400>
- [30] Z. A. Alothman, Low cost biosorbents from fungi for heavy metals removal from wastewater, *Sep. Sci. Technol.*, 55 (2020) 1766–1775. <https://doi.org/10.1080/01496395.2019.1608242>
- [31] F. Almomani, R. Bhosale, M. Khraisheh, T. Almomani, Heavy metal ions removal from industrial wastewater using magnetic nanoparticles (MNP), *Appl. Surf. Sci.*, 506 (2020) 144924. <https://doi.org/10.1016/j.apsusc.2019.144924>
- [32] S. Bahah, S. Nacef, D. Chebli, A. Bouguettoucha, B. Djellouli, A new highly efficient algerian clay for the removal of heavy metals of Cu (II) and Pb (II) from aqueous solutions: characterization, Fractal, kinetics, and isotherm analysis, *Arab. J. Sci. Eng.*, 45 (2020) 205–218. <https://doi.org/10.1007/s13369-019-03985-6>
- [33] E. C. Nnadozie, P. A. Ajibade, Data for experimental and calculated values of the adsorption of Pb (II) and Cr (VI) on APTES functionalized magnetite biochar using Langmuir, Freundlich and Temkin equations, *Data brief.*, 32 (2020) 106292. <https://doi.org/10.1016/j.dib.2020.106292>
- [34] T. C. Umeh, J. K. Nduka, K. G. Akpomie, Kinetics and isotherm modeling of Pb (II) and Cd (II) sequestration from polluted water onto tropical ultisol obtained from Enugu Nigeria, *Applied Water Sci.*, 11(2021) 65. <https://doi.org/10.1007/s13201-021-01402-8>
- [35] S. Tonk, L. E. Aradi, G. Kovács, A. Turza, E. Rápó, Effectiveness and characterization of novel mineral clay in Cd²⁺ adsorption process: Linear and non-linear isotherm regression analysis, *Water*, 14 (2022) 279. <https://doi.org/10.3390/w14030279>
- [36] K. S. Obayomi, M. Auta, A. S. Kovo,

- Isotherm, kinetic and thermodynamic studies for adsorption of lead (II) onto modified Aloji clay, *Desalin. Water Treat.*, 181(2020) 376–384. <https://doi.org/10.5004/dwt.2020.25142>
- [37] A. Benmessaoud, D. Nibou, E. H. Mekatel, S. Amokrane, A comparative study of the linear and non-linear methods for determination of the optimum equilibrium isotherm for adsorption of Pb^{2+} ions onto Algerian treated clay, *Iran. J. Chem. Chem. Eng.*, 39 (2020) 153–171. <https://doi.org/10.30492/IJCCE.2019.35116>
- [38] A. Samad, M. I. Din, M. Ahmed, Studies on batch adsorptive removal of cadmium and nickel from synthetic waste water using silty clay originated from Balochistan–Pakistan, *Chin. J. Chem. Eng.*, 28 (2020)1171–1176. <https://doi.org/10.1016/j.cjche.2019.12.016>
- [39] M. Osanloo, Validation of a new and cost-effective method for mercury vapor removal based on silver nanoparticles coating on micro glassy balls, *Atmos. Pollut. Res.*, 8 (2017) 359-365. <https://doi.org/10.1016/j.apr.2016.10.004>
- [40] A. Samad, M. I. Din, M. Ahmed, S. Ahmad, Synthesis of zinc oxide nanoparticles reinforced clay and their applications for removal of Pb (II) ions from aqueous media, *Chin. J. Chem. Eng.*, 32 (2021) 454–461. <https://doi.org/10.1016/j.cjche.2020.09.043>